

Original Research

High MEIS3 Expression Indicates a Poor Prognosis for Patients with Stage II/III Colorectal Cancer

Jian Ma^{1,†}, Haitao Li^{2,†}, Qianqian Gao³, Weixing Zhang⁴, Changhong Zhu⁵, Jian Chen², Yang Ling¹, Xin Shao^{6,*}, Ziyang Li^{3,*}¹Department of Oncology, Changzhou Tumor Hospital, 213032 Changzhou, Jiangsu, China²Department of Oncology, The Affiliated Yantai Yuhuangding Hospital of Qingdao University, 264000 Yantai, Shandong, China³Department of Pathology, Changzhou Tumor Hospital, 213032 Changzhou, Jiangsu, China⁴Department of Gastrointestinal Surgery, Changzhou Tumor Hospital, 213032 Changzhou, Jiangsu, China⁵Department of Gastroenterology, Changzhou Tumor Hospital, 213032 Changzhou, Jiangsu, China⁶Department of Pathology, Changzhou Hospital of Traditional Chinese Medicine, 213003 Changzhou, Jiangsu, China*Correspondence: 769784185@qq.com (Xin Shao); lzy19871101@163.com (Ziyang Li)

†These authors contributed equally.

Academic Editor: Fu Wang

Submitted: 16 May 2023 Revised: 22 August 2023 Accepted: 4 September 2023 Published: 15 December 2023

Abstract

Background: The Wnt/ β -catenin signaling pathway plays crucial roles in tumor budding and the epithelial–mesenchymal transition (EMT). Myeloid ecotropic viral insertion site 3 (MEIS3)—a direct target of Wnt/ β -catenin—promotes vagal neural crest cell migration into the gut tissue during development; however, its role in cancer progression remains unclear. In this study, the role of MEIS3 in colorectal cancer (CRC) progression was investigated. **Methods:** We analyzed the association between MEIS3 protein expression and the clinical stages of CRC patients, and the effect on tumor cell migration and invasion by wound healing and transwell assays. Finally, we analyzed the association between MEIS3 expression and the disease-free survival (DFS) and overall survival of CRC patients through Kaplan–Meier analysis. **Results:** We found that MEIS3 expression was strongly associated with CRC progression and could be employed to assess DFS in postoperative patients. MEIS3-positive cells were mainly distributed in the growth front and tumor–stroma interface of the CRC tissues, which contain abundant EMT-active and tumor budding cells dominating cancer metastasis. Moreover, MEIS3 promoted CRC cell migration and invasion by regulating effectors including laminin subunit beta 1, matrix metalloprotein 2, and vimentin. MEIS3 protein expression increased with CRC progression according to the clinical stage, which could be used as a biomarker to stratify CRC patients. The 5-year DFS of MEIS3-high patients was poorer than that of MEIS3-low patients (40.6% vs. 61.7%; $p < 0.0001$). Moreover, the 5-year DFS of stage II patients with MEIS3-high expression (53.4%) was comparable to that of stage III patients with MEIS3-low expression (49.5%), while the 5-year DFS of MEIS3-high patients in stage III (30.9%) was comparable to that of stage IV patients (29.6%). **Conclusions:** This study showed that MEIS3 can promote cancer cell metastasis and thus may be a promising biomarker for higher rates of recurrence in postoperative patients with stage II/III CRC.

Keywords: colorectal cancer; recurrence biomarker; disease-free survival; MEIS3; metastasis

1. Introduction

In recent decades, radical surgical resection and subsequent adjuvant radiotherapy and chemotherapy have been the most important treatments for patients with colorectal cancer (CRC) [1,2]. Clinicians mainly rely on magnetic resonance imaging (MRI), positron emission tomography (PET), clinical staging, metastasis, pathological grading of cancer tissue, gene stability, and other indicators before deciding whether to perform adjuvant chemotherapy, targeted therapy, palliative treatment, or other measures on patients [1,3–6]. However, it is difficult to identify early micrometastases with these clinical indicators. As a result, some patients with metastatic cancer fail to receive the appropriate intervention. At least 50% of patients have *in situ* and/or distant metastasis in the liver, lung, and other tissues 2–5 years after surgery, although 25% of patients with

CRC have already undergone clinical metastases at the time of diagnosis or surgical resection [7,8]. Cancer metastasis and recurrence have always been the dominant reason for mortality in CRC patients [9].

Tumor budding is the detachment of single cells or small clusters of no more than five cancer cells from the main tumor mass, and predominantly enters the invasion frontier of the tumor stroma [10,11]. This type of cell disconnects from the bulk cells of the tumor body, degrades the surrounding matrix, migrates away from the tumor body, and becomes the component cell of the invasion front. As a result, tumor budding cells spread to the peripheral circulatory system through lymphatic infiltration, which causes distant metastases and postoperative recurrence [10,12]. Tumor budding and the epithelial–mesenchymal transition (EMT) control how differentiated cancer cells change from having stable properties to ac-



tively invasive behavior. These invasive behaviors are the leading events of cancer metastasis, which then dominates the process of cancer recurrence [13–15]. According to the results of a study by Müller *et al.* [16], tumor budding and related genes indicate a worse clinical prognosis and can be used as important markers for clinical decision-making, especially for patients with stage II CRC [11,16].

During the EMT and tumor budding processes, Wnt/ β -catenin-regulated factors and downstream genes play essential and crucial roles [13,17]. Upon transition from bulk cell to tumor budding, β -catenin translocates from the cell membrane to the cytoplasm followed by Wnt activation [10,13]. After translocation from the cell membrane to the nucleus, β -catenin forms a complex with Wnt protein and binds to the promoter region of target genes to regulate the expression of genes that induce cell invasion such as matrix metalloproteinases (MMPs) [17,18]. Multiple transcription factors, including three-amino-acid-loop-extension homeobox (TALE) proteins, are required to form transcription complexes with Wnt and/or β -catenin to promote cell migration and invasion.

The TALE family consists of myeloid ecotropic viral insertion site (MEIS) and the pre-B cell leukemia transcription factors (PBXs) [19]. The MEIS family includes *MEIS1*, *MEIS2*, *MEIS3*, *Prep1*, and *Prep2* genes, which are essential for embryonic development and cancer progression [19,20]. *MEIS3* is expressed in spatial and temporal patterns and is essential for early embryonic development [20,21]. As a target gene of Wnt/ β -catenin, *MEIS3* promotes posterior neural cell migration into the hindbrain and gut tissues [21–23]. Hirschsprung's disease, a hereditary disorder with congenital megacolon as its primary symptom, is caused by *MEIS3* deficiency and affects children and newborns [24]. Although there have been reports about the role of *MEIS3* in hepatocellular carcinoma and glioma, whether and how *MEIS3* participates in the progression of gut tumors is currently unknown [25,26].

Based on the function of *MEIS3* in the gut and cancer development, we hypothesized that *MEIS3* may be crucial for CRC metastasis, recurrence, and survival. Thus, we investigated the *MEIS3* expression pattern in CRC tissues, as well as the relationship with CRC progress in the clinic. We also analyzed the role of *MEIS3* in CRC cell metastasis. Furthermore, we stratified the patients by protein level and clinical stage to confirm the value of *MEIS3* as a prognostic biomarker for CRC recurrence after radical resection.

2. Materials and Methods

2.1 Clinical Samples

This study was approved by the ethics committee of the Changzhou Tumor Hospital (Changzhou, China). The consent form was signed by patients according to the International Ethical Guidelines for Human Biomedical Research standards. The clinical staging of CRC patients was carried out following the American Joint Committee

on Cancer (AJCC) standard, meaning that clinical staging was based on cancer tissue invasion, lymph node metastasis, and distal metastasis [1]. All patients were treated according to the CRC guidelines of the Chinese Society of Clinical Oncology. During follow-up, once recurrence was found, it was recorded as the endpoint of disease-free survival (DFS). If the patient died for any reason other than CRC, the data were deleted. From 2015 to 2020, a total of 323 patients participated in the study, and 292 patients were ultimately included in the analysis (**Supplementary Table 1**). Cancer and paracancer tissues from patients were treated with liquid nitrogen for at least 1 h before being stored at -80°C for subsequent Western blotting (WB) and immunohistochemistry (IHC) analyses.

2.2 Antibodies, Cell, and Culture Medium

In this study, we used the following antibodies: rabbit anti-*MEIS1* (1:500; Atlas Antibodies, Bromma, Sweden), rabbit anti-*MEIS2* (1:500; Proteintech Group, Rosemont, IL, USA), rabbit anti-*MEIS3* (1:500 for WB, 1:100 for IHC; Atlas Antibodies), rabbit anti-laminin beta 1 (anti-LamB1) (1:500; Proteintech Group), rabbit anti-MMP2 (1:500; Proteintech Group), rabbit anti-E-cadherin (1:1000; Cell Signaling Technology [CST], Danvers, MA, USA), mouse anti-beta catenin (ACTB, 1:1000; Proteintech Group), mouse anti-vimentin (VIM, 1:2000; Proteintech Group), rabbit anti-ACTB (1:3000; Proteintech Group), horseradish peroxidase (HRP)-conjugated Affinipure Donkey Anti-Mouse IgG (H+L) (1:5000; Proteintech Group), HRP-conjugated donkey anti-rabbit IgG (H+L) (1:5000; Proteintech Group), rabbit anti-E-cadherin (1:500; Thermo Fisher Scientific, Waltham, MA, USA), and mouse anti-vimentin (1:500; CST). Dulbecco's Modified Eagle Medium (DMEM) and fetal bovine serum for cell culture were purchased from Thermo Fisher Scientific. The CRC strains SW480 and SW1116 were from Shanghai ZJ Bio-Tech Co., Ltd. (Shanghai, China) and Fuheng Biology Co., Ltd. (Shanghai, China). All cell lines were validated by STR profiling and tested negative for mycoplasma. Cells were all cultured in a humidified incubator at 37°C and 5% CO_2 .

2.3 Quantitative Polymerase Chain Reaction (PCR) and WB

The total RNA in cells was extracted with the Trizol method, and reverse transcription was performed with AMV Reverse Transcriptase (Promega, Madison, WI, USA). Quantitative PCR (qPCR) was performed using a SYBR Green PCR Master Mix (Toyobo, Tokyo, Japan) according to the manufacturer's instructions. The $2^{-\Delta\Delta\text{Ct}}$ method was used to quantify gene expression. The detailed methods and primers for qPCR are shown in **Supplementary Methods** and **Supplementary Table 2**, respectively.

Protein extraction and WB were carried out according to the protocols described in *Molecular Cloning: A Lab-*

oratory Manual, with modification [27]. Briefly, RIPA buffer was used to lyse the tissues or cells, and the Bradford method was used to quantify the protein. After boiling in Laemmli buffer for 10 min, protein samples were resolved on a 10% sodium dodecyl sulfate polyacrylamide gel electrophoresis gel, followed, and electrophoretically transferred to a PVDF membrane. After blocking in 5% fat-free milk powder in Tris-buffered saline with 0.1% Tween20 detergent (TBST) for 30 min, the membrane was incubated with primary antibody overnight at 4 °C. The next day, the membrane was washed three times with TBST for 5 min, and then incubated with a secondary antibody at a dilution of 1:5000 at room temperature for 2 h. The film was scanned after developing, and its gray-scale value was analyzed using Quantitative One 4.40 software to evaluate the relative protein expression. The ratio = (MEIS3c/ACTBc)/(MEIS3p/ACTBp) was employed to determine the protein abundance of MEIS3 in the CRC tissue, and the ratio = (target/ACTB) was used to determine the abundance of the target protein in the cell sample.

2.4 Immunohistochemistry (IHC)

The tissues were dehydrated in various alcohol concentrations (i.e., 70%, 80%, 95%, 100%, and 100%), made transparent with xylene, fixed in 4% paraformaldehyde, and finally embedded in paraffin wax for 24 h. Then slices were prepared by cutting the tissues at a thickness of 8 μm using a microtome (Leica, Wetzlar, Germany). The tissue samples were reverse-treated with 100% to 50% alcohol from xylene, dipped in sodium citrate antigen repair solution, and repaired with the microwave method. Following a 10-min soak in 5% hydrogen peroxide, the tissue samples were rinsed under running water for 1 min before being incubated in 10% rabbit serum for 1 h. Then the serum was replaced with MEIS3 antibody (1:100) and incubated overnight at 4 °C. The next day, slices were washed three times with phosphate-buffered saline (PBS) and incubated in HRP-conjugated IgG (1:500) for 1 h at room temperature. The color was developed with the SABC method. Slices were sealed with neutral gum after being dehydrated with a gradient of ethanol and xylene, and the images were photographed using a microscope.

2.5 Construction of Virus Particles

The lentiviral particles for MEIS3 silencing were packaged with the assistance of Shanghai ZJ Bio-Tech Co., Ltd. The knockdown expression vector was composed of three U6 promoters connected in series, each of which directed a short hairpin MEIS3 RNA (shMEIS3) sequence. The three shRNA sense sequences were as follows: 5'-CUUGGAAGGAGAAUGGCAUUAUUCTA-3', 5'-CUGCAAGUCAACAACUGGUUCAUTA-3', and 5'-CUGGUGGAGAAGAUGAGGACUUGGA-3'.

2.6 Transwell Migration Assay

The cells were first cultured in DMEM without FBS for 24 h. During this time, the Transwell chambers were soaked and moistened with 1 × PBS. Then matrigel was added and incubated in a CO₂ incubator at 37 °C to congeal the gel. Next, the lower chamber was filled with 600 μL complete medium containing FBS and 200 μL cell suspension (density 5 × 10⁵ cells/mL) was added to the upper chamber, followed by incubation for 24 h. Cells that migrated to the lower surface of the membrane were fixed, stained with 0.5% crystal violet, and counted under a microscope.

2.7 Public Database Data

The patient's MEIS3 mRNA level, DFS, and overall survival (OS) analysis of The Cancer Genome Atlas (TCGA) database were performed on the Gene Expression Profiling Interactive Analysis (GEPIA) portal (<http://gepia.cancer-pku.cn/>) [28]. The data of GSE17537 in the Gene Expression Omnibus (GEO) database was downloaded from GenomicScape (<http://www.genomicscape.com/>) and analyzed again with GraphPad Prism 8.0 (GraphPad Software, San Diego, CA, USA) [29,30]. Independent OS analysis was also implemented on this platform.

2.8 Statical Analyses

For statistical analyses, we used GraphPad Prism 8.0 (GraphPad Software, Boston, MA, USA). To examine the differences between comparisons in protein level, cell migration, and invasion, the *t*-test and/or one-way analysis of variance were utilized. The 5-year DFS and OS of patients with different factors were estimated with Kaplan–Meier curves and log-rank tests.

3. Results

3.1 MEIS3 Localization in CRC Tissues

First, we analyzed the localization pattern of MEIS3-positive cells in CRC tissues by IHC. Although regulated by Wnt/β-catenin protein, the distribution pattern of MEIS3-positive cells was not consistent with the characteristics of β-catenin [31]. As shown in Fig. 1, MEIS3 protein was not found in bulk cells, which were well differentiated (Fig. 1A,B) but were present in the cell nucleus of the cancer invasion front (Fig. 1C,D). The invasion fronts dominate the process of cancer invasion into paracancer and then metastasis into distant organs [10]. The second regions containing abundant strong MEIS3-positive cells were the tumor–stroma interface (Fig. 1E,F), which was similar to VIM in tumor budding [32,33]. By morphological characteristics, we found tumor budding cells in these MEIS3-positive cells, which have active migration ability (Fig. 1D,F). MEIS3-positive cells were also widespread in undifferentiated regions composed of cells that proliferate vigorously (Fig. 1G,H), yet the staining intensity was much

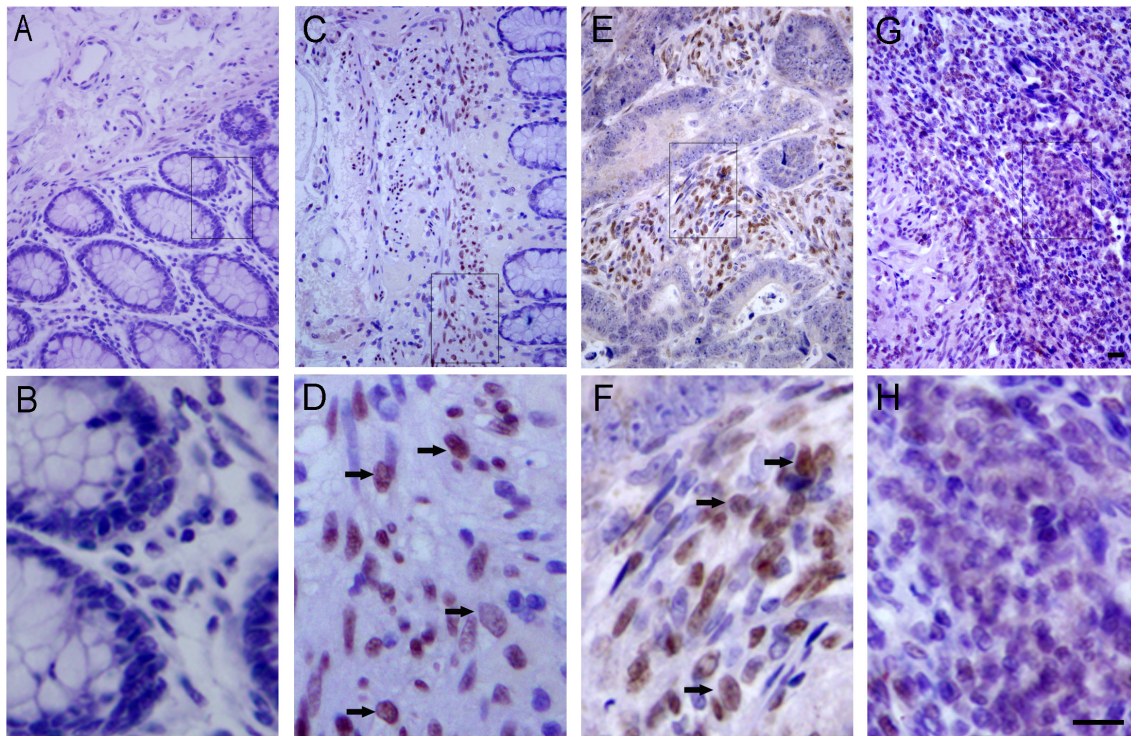


Fig. 1. Localization of myeloid ecotropic viral insertion site 3 (MEIS3) protein in colorectal cancer (CRC) tissues. MEIS3 was not detected in well-differentiated CRC tissue areas (A,B) but was detected in the cancer nucleus of the growth front (C,D) and tumor–stroma interface regions (E,F) containing an abundance of budding cells (black arrows, D, F), and was widely distributed in poorly differentiated cells, although the intensity was weak (G,H). Among them, B, D, F, and H are the screenshots within the boxes of A, C, E, and G diagrams, respectively. Scale bar = 50 μ m.

weaker than the invasion fronts and tumor–stroma interface (Fig. 1C–F). Thus, the IHC results suggest that MEIS3 is related to tumor budding cells.

3.2 Association between MEIS3 Expression and CRC Progression

We employed the ratio of protein abundance between cancer and paracancer to evaluate MEIS3 protein expression. We found that the MEIS3 expression was significantly increased in CRC compared to paracancer (2.81 ± 1.45 fold; $p < 0.01$) (Fig. 2A,B), which incrementally increased with CRC progression (stage I/stage II/stage III/stage IV: $1.71 \pm 0.94/2.52 \pm 0.97/3.16 \pm 1.43/3.42 \pm 1.31$ fold, respectively; $p < 0.01$) (Fig. 2C). Considering the association between clinical stage and cancer metastasis, we used clinical stage as an indicator of CRC metastasis.

To verify the results, we employed the GSE4107 cohort data to analyze MEIS3 expression in CRC tissues [34]. As shown in Fig. 2D, MEIS3 mRNA expression in cancer tissues was significantly increased to about 3 fold that in normal control tissue ($p = 0.015$). By employing the GEPIA platform, we found that MEIS3 mRNA levels gradually increased with clinical staging progression (Fig. 2E). Although the expression of some genes was found to be sex-related, we did not find this trend for MEIS3 in our

cohort (female vs. male: 2.86 ± 1.29 vs. 3.05 ± 1.19 ; $p = 0.43$) (Fig. 2F). Considering the relationship between clinical stage and cancer metastasis, these results show that MEIS3 expression is positively correlated with the progression of CRC metastasis.

3.3 MEIS3 Enhances CRC Cell Metastasis

Based on the distribution characteristics of MEIS3-positive cells (Fig. 1), the correlation between MEIS3 expression and CRC progression in tissues (Fig. 2), and the role of MEIS3 in promoting cell migration into gut tissue, we hypothesized that MEIS3 may contribute to CRC cell migration and invasion [22,23]. We constructed lentiviral particles carrying three tandem U6-promoter-MEIS3-shRNA, which were employed to silence MEIS3 expression in SW480 and SW1116 cells (Supplementary Fig. 1A). By analyzing the mRNA and protein levels of MEIS1, MEIS2, and MEIS3, we determined that the virus particle could specifically and effectively silence MEIS3 expression (Supplementary Fig. 1B–E, Supplementary Table 2).

The scratch wound healing assay was used to analyze cell migration ability. When the wound area of the SW480 cells was covered by $67.1 \pm 7.82\%$, only $34.3 \pm 4.73\%$ of the region was covered by MEIS3-silenced cells ($p < 0.001$; Fig. 3A). The migrated area of SW1116 cells was also sig-

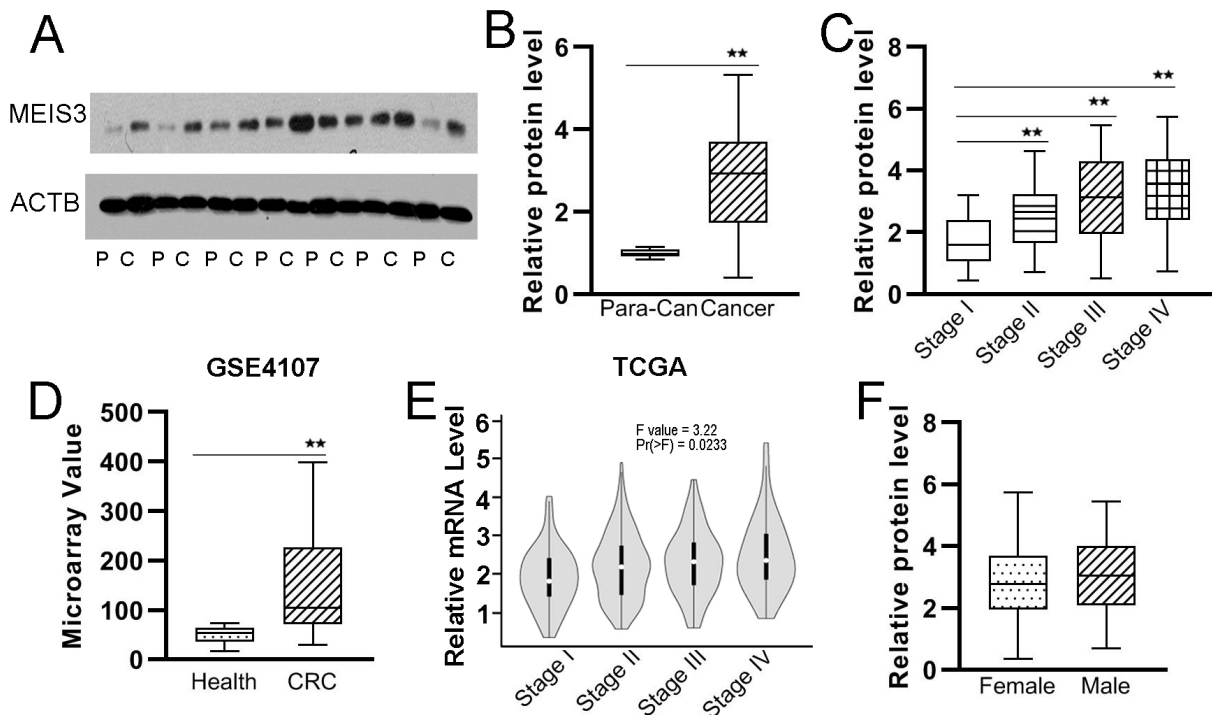


Fig. 2. Expression level of MEIS3 in CRC. The MEIS3 protein expression in CRC cancer and paracancer tissues was detected by Western blotting (WB) (A) based on which we analyzed the ratios of MEIS3 protein abundance in CRC tissues to paracancer tissues in our cohort (B) and GSE4107 cohort (D) and the tendency of MEIS3 expression in cancer tissues according to clinical stage in our cohort (C) and The Cancer Genome Atlas (TCGA) cohort (E). The relative protein expression of MEIS3 in CRC tissues was also analyzed according to sex (F). P, Paracancer tissue; C, Cancer tissue. $**p < 0.01$.

nificantly decreased in MEIS3-silenced cells (wound area closure, shCTL vs. shMEIS3: $63.7 \pm 5.12\%$ vs. $41.5 \pm 3.10\%$; $p < 0.001$) (**Supplementary Fig. 2B**).

The invasion process of cancer cells relies on degrading the surrounding matrix and penetrating adjacent tissues; thus, we employed Matrigel-covered transwells to analyze the role of MEIS3 in invasion. When MEIS3 was silenced, the penetration level of SW480 cells was reduced by 61.8% (Transwell cell number, shCTL vs. shMEIS3: 101.3 ± 6.03 vs. 38.7 ± 3.05 ; $p < 0.001$) (Fig. 3B). The same treatment reduced the invasion level of SW1116 cells by 44.2% (shCTL vs. shMEIS3: 97.3 ± 5.03 vs. 54.3 ± 6.11 ; $p < 0.001$) (**Supplementary Fig. 2B**). Thus, MEIS3 silencing significantly reduced the migration and invasion ability of CRC cells.

We analyzed the protein expression of LamB1, E-Cadherin, VIM, MMP2, and β -catenin, which are responsible for the migration and invasion of tumor cells in the EMT and tumor budding process [13,17,33]. We found that LamB1, VIM, and MMP2 expression was significantly decreased; E-Cadherin expression was increased; and β -catenin expression did not significantly change upon MEIS3 silencing (Fig. 3C, **Supplementary Fig. 2C**). Therefore, high MEIS3 expression may increase CRC metastasis by enhancing tumor budding and/or the EMT.

Then we made an expression association analysis between MEIS3 and genes that regulate cancer cell metastasis and proliferation in TCGA cohort on the GEPIA platform [28]. MEIS3 expression was positively correlated with genes promoting cell migration and invasion such as VIM ($R = 0.78$; $p < 0.001$), MMP2 ($R = 0.71$; $p < 0.001$), fibronectin (FN1) ($R = 0.63$; $p < 0.001$), and LamB1 ($R = 0.15$; $p = 0.013$); genes regulating the EMT and tumor budding process including Twist-related protein 1 (TWIST1) ($R = 0.66$; $p < 0.001$), TWIST2 ($R = 0.72$; $p < 0.001$), Snail family transcriptional repressor 1 (SNAI1) ($R = 0.53$; $p < 0.001$), SNAI2 ($R = 0.71$; $p < 0.001$), and transforming growth factor beta ($R = 0.77$; $p < 0.001$). However, there was a weak or even no correlation with the genes regulating cell proliferation including cyclin D1 ($R = 0.15$; $p = 0.011$), proliferating cell nuclear antigen ($R = -0.12$; $p = 0.023$), and MYC ($R = -0.1$; $p = 0.083$) (**Supplementary Fig. 3**). These results suggest that MEIS3 might lead to cancer metastasis by regulating the migration and invasion abilities of CRC cells.

3.4 High MEIS3 Expression is Correlated with a Poor Prognosis in CRC Patients

Based on the MEIS3 protein ratio of cancer/paracancer, CRC patients were stratified into two groups with

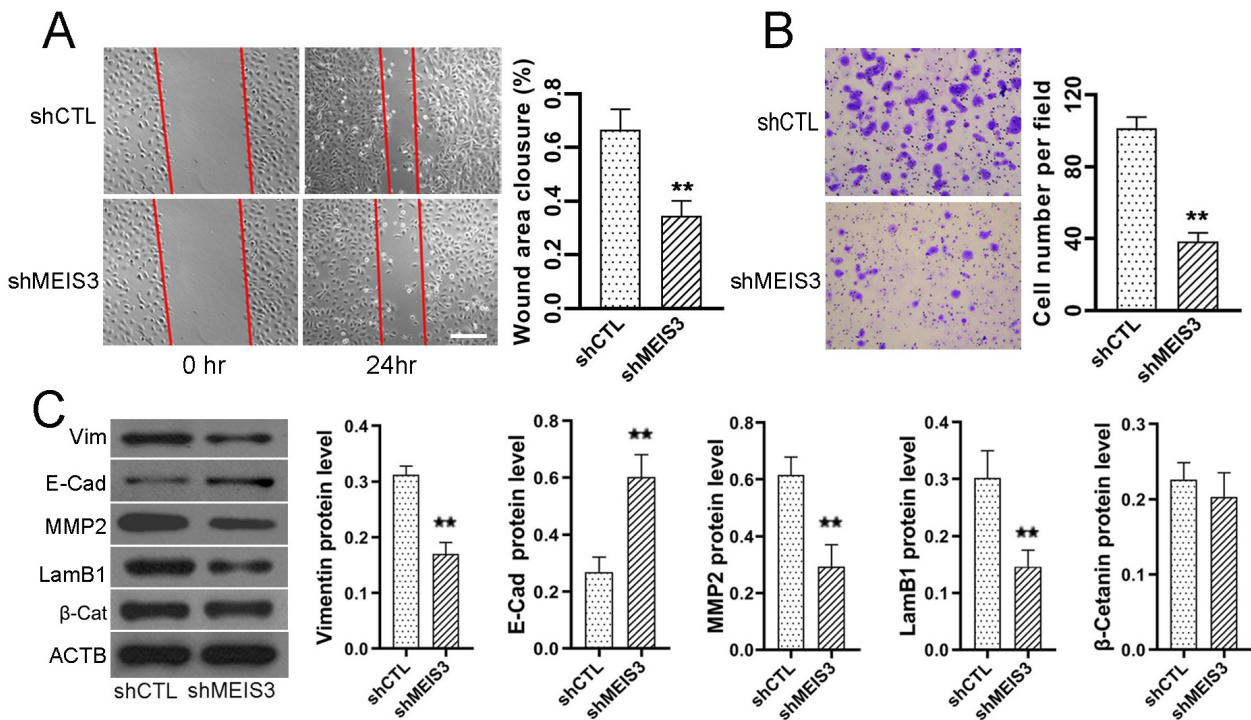


Fig. 3. Silencing of MEIS3 expression results in a significant decrease in SW480 cell metastasis. After treatment with lentivirus particles expressing negative control shRNA or shMEIS3, we analyzed the wound closure area of SW480 cells (A) with the scratch wound healing assay, and crystal violet-stained SW480 cells (B) in transwell analysis and counted the cells. MEIS3 silencing also resulted in the decreased protein expression of VIM, LamB1, and MMP2, and increased expression of E-cadherin in SW480 cells (C). ** $p < 0.01$. Scale bar = 200 μm .

equal numbers. We used the Kaplan–Meier curve to analyze the 5-year DFS of CRC patients. As shown in Fig. 4A, the 5-year DFS of MEIS3-high and MEIS3-low cohorts were 61.7% and 40.6%, respectively (hazard ratio [HR] = 2.441, 95% confidence interval [CI]: 1.493–3.989; $p < 0.0001$) (Fig. 4A, Table 1). However, when grouped by sex, age, tumor volume, or location, the 5-year DFS of patients did not show significant differences (Supplementary Table 1).

To verify these results, we analyzed the DFS of CRC patients from TCGA cohort on the GEPIA platform [28]. The 5-year DFS of the MEIS3-high cohort was significantly lower than that of the MEIS3-low cohort with a cutoff of 50% ($p = 0.0026$; Fig. 4B). Then we analyzed the GSE17537 cohort from the GEO database and found the same trend ($p = 0.0073$; Fig. 4C). Therefore, MEIS3 can be employed to independently assess the recurrence risk of CRC patients after surgery.

We also analyzed the 5-year OS rate grouped as the 5-year DFS. The 5-year OS of the MEIS3-high cohort was 42.6%, which was significantly lower than that of the MEIS3-low cohort (62.3%; $p < 0.001$) (Fig. 4D). Regarding TCGA cohort, the 5-year OS of the MEIS3-high cohort was also significantly lower than that of the MEIS3-low co-

hort with a cutoff of 45% ($p = 0.0084$; Fig. 4E). Another independent survival analysis of the GSE17537 cohort also showed similar results ($p = 0.00012$; Fig. 4F). In conclusion, high MEIS3 expression was strongly correlated with a poor prognosis in CRC patients.

3.5 High MEIS3 Expression Indicates Recurrence Risk in Patients with Stage II/III Disease

Currently, the prognosis for the postoperative recurrence of CRC is predominantly based on clinical stage [1]. We determined whether a more precise prognosis could be made when MEIS3 expression is introduced into the prognosis system. To this end, we performed multivariate analysis according to MEIS3 expression with The American Joint Committee on Cancer (AJCC) stage and other independent factors (Table 1). As shown in Fig. 5, the 5-year DFS of the stage II MEIS3-high cohort was significantly lower than that of the MEIS3-low cohort (53.4% vs. 67.3%, HR = 2.38, 95% CI: 0.9843–5.786; $p = 0.0123$) (Table 1, Fig. 5B). The 5-year DFS of the stage III MEIS3-high cohort was also significantly lower than that of stage III MEIS3-low cohort (30.9% vs. 49.5%, HR = 2.817, 95% CI: 1.370–5.792; $p = 0.0038$) (Table 1, Fig. 5C). Moreover, the 5-DFS was comparable between the stage II MEIS3-high cohort and

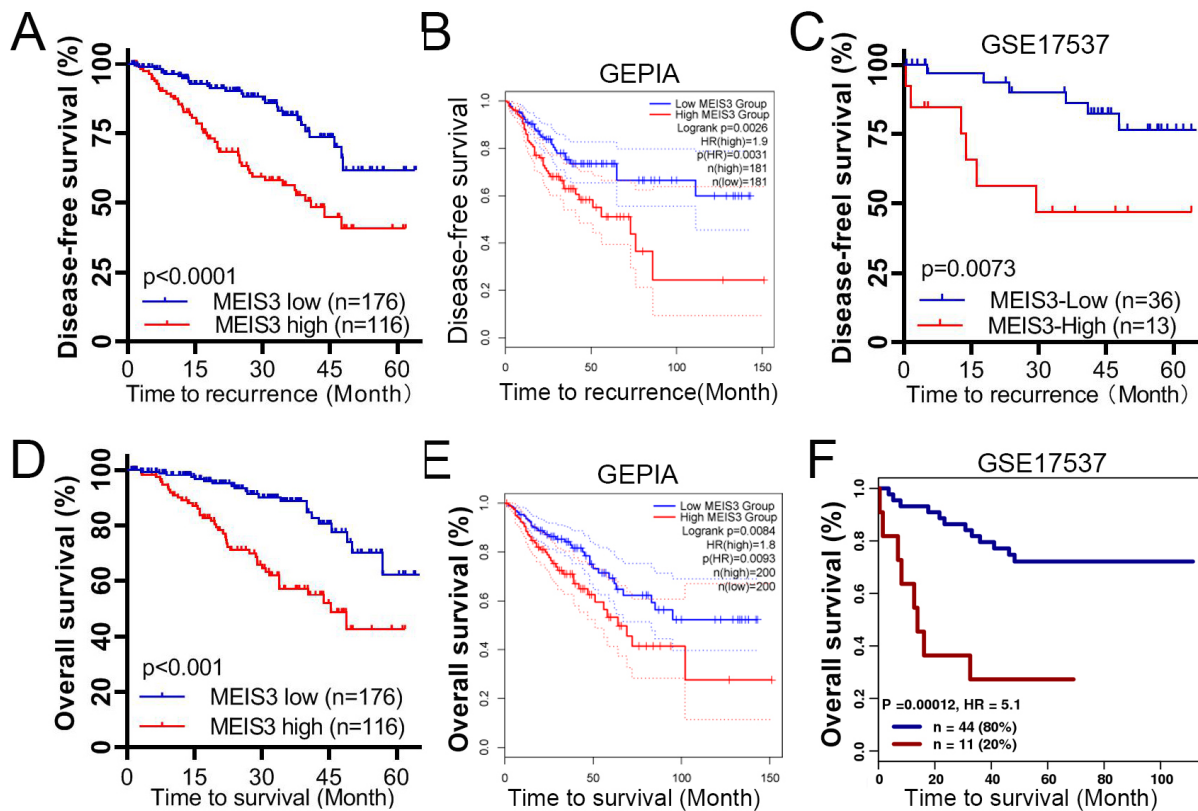


Fig. 4. Disease-free survival (DFS) and MEIS3 level in CRC patients. The 5-year DFS of our cohort was stratified by MEIS3 level (A) and verified through independent analysis in the Gene Expression Profiling Interactive Analysis (GEPIA) portal (B) and GSE17537 dataset (C). The relationship of 5-year OS of patients and MEIS3 level are shown from our cohort (D), GEPIA platform of TCGA cohort (E), and GSE17537 by GenomicScape portal (F). The blue line indicates the MEIS3-low group, and the red line indicates the MEIS3-high group.

stage III MEIS3-low cohort (53.4% vs. 49.5%; $p = 0.23$) (Fig. 5E), and between the stage III MEIS3-high cohort and overall stage IV cohort (29.6% and 30.9%; $p = 0.7844$) (Fig. 5F). However, when grouped by MEIS3 expression, there was no prognostic difference in the sub cohort of stage I and IV patients (Fig. 5A,D, Table 1).

4. Discussion

It is well known that budding and the EMT are common mechanisms in organ development and tumor progression, and play essential roles under orderly regulation [32,35,36]. Genes that guide cell migration in organ development also tend to regulate cancer progression. MEIS3 is responsible for promoting neural cell migration into gut tissue during embryonic development [23]. Clinical cases show that the genetic deletion of chromosome 19q13.32 region containing MEIS3 leads to Hirschsprung's disease, a birth defect of the intestines caused by a congenital developmental disorder [24].

Here, we found that MEIS3 is overexpressed in the invasion front of CRC tissues, especially in tumor bud-

ding cells presenting with high metastasis activity [23,33]. MEIS3 is also highly overexpressed in tumor stroma, which is consistent with the expression characteristics of VIM [32,37]. High expression of VIM promotes cell invasion, which is one of the hallmark events of both the EMT and tumor budding [37]. Although the transcription of MEIS3 is inhibited by the protein that has been produced, we found that MEIS3 expression increased with metastatic CRC progression in the CRC and TCGA cohorts [38]. The biomarkers and results of our cohort and TCGA cohort were different, yet they all gradually increased with the decrease in cancer metastasis. Therefore, MEIS3 expression may reflect the metastasis potential in CRC tissue.

MEIS3 is essential for the migration of nerve cells in embryonic gut development [22,23]. The migration and invasion abilities of CRC cells were significantly reduced upon MEIS3 silencing, confirming the value of this gene in cancer metastasis. These results were also consistent with the MEIS3 expression pattern in CRC tissues, meaning that the IHC signal intensity of MEIS3 in cells with high metastatic activity was stronger than that in active proliferation cells and negative in differentiated tumor stroma cells.

Table 1. Multivariate analyses of risk factors for DFS.

Variables	MEIS3 High/Low	Percent (%)	5-Year DFS (%)	Hazard ratio	95% CI	p-value
Age (years)						
<57	72/91	55.8	46.3/68.9	3.259	1.634–6.499	0.0008
>57	44/85	41.2	36.3/53.9	2.245	1.150–4.384	0.0075
Sex						
Male	64/89	52.4	28.1/66.5	2.924	1.520–5.628	0.0005
Female	52/87	47.6	54.2/55.2	1.992	1.004–3.951	0.0378
Position						
Colon	62/114	60.3	37.8/67.9	2.812	1.453–5.443	0.0006
Rectum	54/62	39.7	45.3/49.2	1.955	0.9900–3.862	0.0491
Tumor size (cm)						
<5	61/104	56.2	51.7/63.3	2.205	1.175–4.140	0.0057
>5	55/72	43.8	28.4/56.1	2.908	1.415–5.974	0.0021
MEIS3 expression						
High	116	39.7	40.6	2.441	1.493–3.989	0.0001
Low	176	60.3	61.7			
AJCC stage						
I	18/29	16.1	82.1/85.7	6.0180	0.4402–82.26	0.0875
II	36/71	36.6	53.4/67.3	2.3870	0.9843–5.786	0.0123
III	43/52	32.5	30.9/49.5	2.8170	1.370–5.792	0.0038
IV	19/24	14.7	29.9/28.7	1.2360	0.4973–3.073	0.6426

CI, confidence interval; AJCC, The American Joint Committee on Cancer.

Among the related biological phenomena and molecular mechanisms, E-cadherin and β -catenin leave the cell membrane, and β -catenin enters the nucleus upon Wnt activation, this is the beginning of the Hulk cell transition to tumor budding or mesenchymal cells [10]. β -catenin directly binds to the MEIS3 promoter region, and Wnt3a is a necessary condition for MEIS3 transcription [21]. Then translated MEIS3 protein participates in DNA-binding complex formation with PBX and/or Hox to control the transcription factor accumulation on the promoter of target genes [22]. Finally, MEIS3 regulates nerve cell migration during gut development by activating Sonic Hedgehog expression, and primary nerve cell differentiation through fibroblast growth factor 3 (FGF3) and FGF8 activity [21,23,35]. In this study, we found that MEIS3 can promote the expression of genes such as VIM, MMP2, and Lamb1, which work as behavioral factors in cell migration and invasion [13,17,32,33]. Moreover, MEIS3 is significantly and positively correlated with MMP2, Vim, Lamb1, and FN1 at high or moderate levels in CRC tissues, suggesting that it may indirectly or directly promote cancer metastasis. Unlike these genes, MEIS3 may not be expressed in bulk cells, indicating that this gene has stronger specificity for regulating the EMT and tumor budding processes.

The survival rate of CRC patients with primary regional diseases has benefited from radical surgical resection; however, distant metastasis often indicates terminal illness and is the primary cause of death [10,39]. The prognostic diagnosis of recurrence risk is mainly based on the

clinical stage, pathological assays, chest X-ray, computed tomography (CT), MRI, and PET, which were the basement to give adjuvant radiotherapy and chemotherapy, targeted drugs, or palliative care [1,2,6,40]. Tumor budding, EMT, and related genes have also been recognized as independent prognostic factors [10,11,14].

When stratifying the postoperative patients by MEIS3 level, we found that the DFS and OS of the MEIS3-high cohort were significantly worse than those of the MEIS3-low cohort. These results were also supported by the cohorts from ATGC and GSE17537 [30]. When we stratified stage II/III patients by MEIS3 level, we found that patients could be regrouped. Among stage II patients, the sub cohort with high MEIS3 expression had a similar recurrence risk as stage III patients with low MEIS3 expression, whereas those with low MEIS3 expression had a recurrence risk closer to stage I patients. Similarly, among stage III patients, the recurrence risk of those with high MEIS3 expression was almost the same as that of overall stage IV patients. Thus, when stratified by MEIS3 protein level and clinical stage, we could detect the patients with higher recurrence risk who would not be discovered by current clinical methods. By contrast, carcinoembryonic antigen, carbohydrate antigen 19-9, and other biomarkers are not more discriminative than clinical staging in predicting recurrence after operation [41,42]. The combination of tumor budding/EMT, functional genes, and clinical stage may effectively screen patients with high recurrence risk.

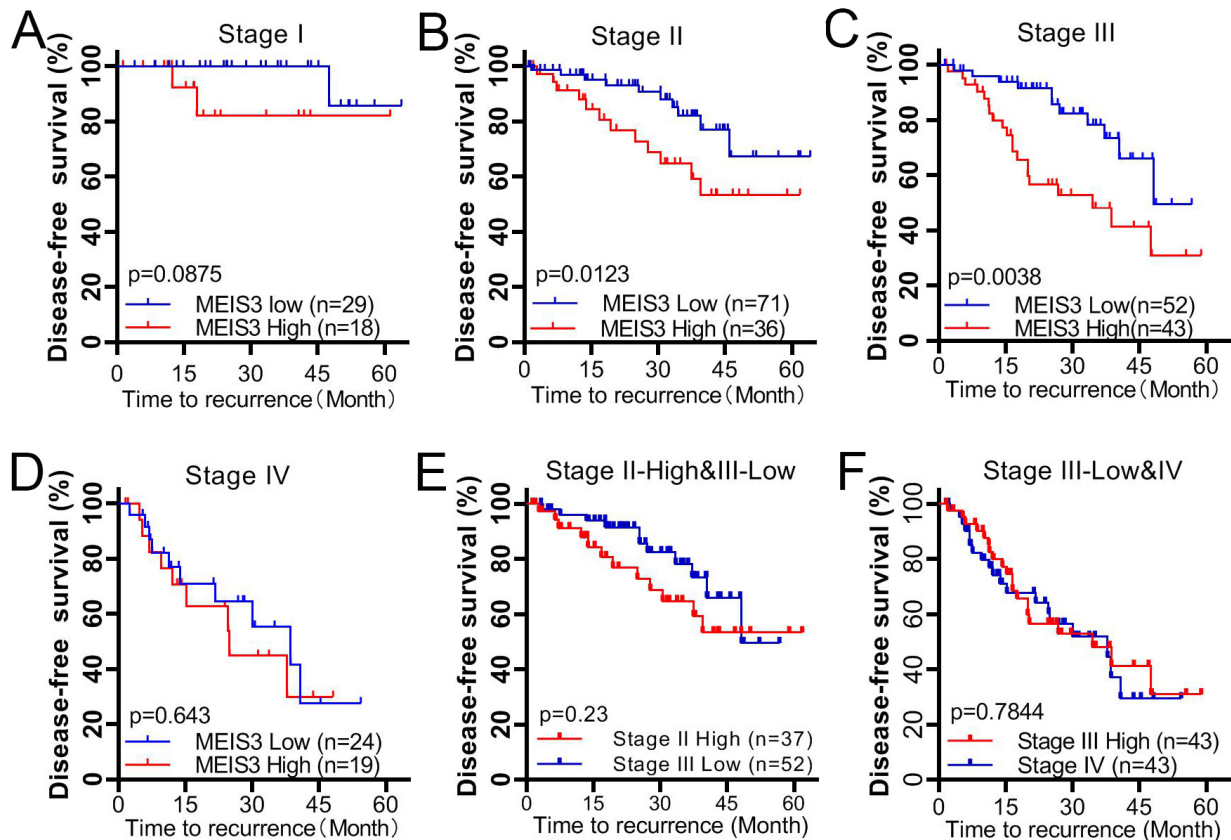


Fig. 5. DFS in different clinical stages of CRC patients. The 5-year DFS of postoperative CRC patients was stratified by MEIS3 expression according to clinical stage I (A), stage II (B), stage III (C), and stage IV (D). Comparison between the stage II MEIS3-high cohort and stage III MEIS3-low cohort (E), and between the stage III MEIS3-high cohort and stage IV cohort (F).

Open databases and analysis platforms such as TCGA and GEO provided abundant clinical and corresponding gene expression data, most of which are mRNA levels based on gene chips and high-throughput sequencing [28, 29]. This allows our research to be based on a more solid and reliable foundation, although the expression of mRNA and protein is not a simple linear relationship. Our research has benefited from these public platforms, but we need a larger retrospective cohort to study the feasibility of MEIS3 as a biomarker for high recurrence risk before this marker can be applied clinically.

We also found that MEIS3 can promote metastasis by activating functional genes such as LamB1, VIM, and FN1, which play crucial roles in the EMT and tumor budding process [17,43]. Yet, we do not know the specific regulation process. Additional studies are needed to determine how MEIS3 regulates these genes to understand the specific roles in tumor budding and/or EMT processes.

5. Conclusions

In summary, we found that MEIS3 plays a crucial role in the tumor budding/EMT of CRC cells, and the high expression of this gene can promote cancer cell

metastasis. The highMEIS3 expression in CRC tissues is strongly associated with cancer progression and indicates a poor recurrence risk for stage II/III patients after radical surgery. MEIS3 is expected to be used as a poor prognostic biomarker for CRC patients in the middle stages. Genes that play important roles in the EMT or tumor budding during development, but are low or even quiescent in normal organs, may provide new insights into understanding CRC metastasis and recurrence.

Abbreviations

CRC, colorectal cancer; MEIS, myeloid ecotropic viral insertion site; DFS, disease-free survival; OS, overall survival; MRI, magnetic resonance imaging; PET, positron emission tomography; EMT, epithelial–mesenchymal transition; TALE, three amino acid loop extension homeobox; PBX, pre-B cell leukemia; MAPK, mitogen-activated protein kinase; CSCO, Chinese Society of Clinical Oncology; WB, Western blotting; IHC, immunohistochemistry; PBS, phosphate-buffered saline; shCTL, short hairpin control RNA; shMEIS3, short hairpin MEIS3 RNA; LamB1, laminin subunit beta 1; MMP2, matrix metalloproteinase 2; ACTB, β -actin; LamB1, laminin subunit beta 1.

Availability of Data and Materials

The datasets used and/or analyzed during the current study are available from the corresponding author on reasonable request.

Author Contributions

JM, ZL, XS, and HL made substantial contributions to the conception or design of the work. QG, WZ, CZ, JC, and YL made substantial contributions to the acquisition, analysis, or interpretation of data for the work. JM and HL wrote the manuscript. All authors contributed to revising the manuscript critically for important intellectual content and final approval of the version to be published. All authors have participated sufficiently in the work and agreed to be accountable for all aspects of the work.

Ethics Approval and Consent to Participate

Written informed consent was obtained from the individual for the publication of any potentially identifiable images or data included in this article. The studies involving human participants were reviewed and approved by the ethics committee of the Changzhou Tumor Hospital (2017-SY-012). The participants provided their written informed consent to participate in this study.

Acknowledgment

We would extend our most sincere gratitude to Ang Li from the School of Life Science and Technology, Tongji University, Shanghai, for his valuable suggestions and help in experimental design and technology.

Funding

This research was funded by Changzhou Sci&Tech Program, China, with grant number CJ20160049.

Conflict of Interest

The authors declare no conflict of interest.

Supplementary Material

Supplementary material associated with this article can be found, in the online version, at <https://doi.org/10.31083/j.fbl2812338>.

References

- [1] Edge SB, Fritz AG, Byrd DR, Greene FL, Compton CC, Andy Trotti I. *AJCC 7th Ed Cancer Staging Manual*. Springer: New York Dordrecht Heidelberg London. 2016.
- [2] China NHCotPsRo. Chinese Protocol of diagnosis and treatment of colorectal cancer (2020 edition). *Zhonghua Wai Ke Za Zhi*. 2020; 58: 561–585. (In Chinese)
- [3] Shi Y, Wang M, Zhang J, Xiang Z, Li C, Zhang J, *et al*. Tailoring the clinical management of colorectal cancer by ¹⁸F-FDG PET/CT. *Frontiers in Oncology*. 2022; 12: 1062704.
- [4] Lin X, Li Y, Wang S, Zhang Y, Chen X, Wei M, *et al*. Diagnostic value of [(68)Ga]Ga-FAPI-04 in patients with colorectal

- cancer in comparison with [(18)F]F-FDG PET/CT. *Frontiers in Oncology*. 2022; 12: 1087792.
- [5] Ren Q, Chen Y, Shao X, Guo L, Xu X. Lymph nodes primary staging of colorectal cancer in 18F-FDG PET/MRI: a systematic review and meta-analysis. *European Journal of Medical Research*. 2023; 28: 162.
- [6] Poston GJ, Tait D, O'Connell S, Bennett A, Berendse S, Guideline Development Group. Diagnosis and management of colorectal cancer: summary of NICE guidance. *BMJ (Clinical Research Ed.)*. 2011; 343: d6751.
- [7] Hansdotter P, Scherman P, Petersen SH, Mikalonis M, Holmberg E, Rizell M, *et al*. Patterns and resectability of colorectal cancer recurrences: outcome study within the COLOFOL trial. *BJS Open*. 2021; 5: zrab067.
- [8] Xu W, He Y, Wang Y, Li X, Young J, Ioannidis JPA, *et al*. Risk factors and risk prediction models for colorectal cancer metastasis and recurrence: an umbrella review of systematic reviews and meta-analyses of observational studies. *BMC Medicine*. 2020; 18: 172.
- [9] Liang Z, Xie H, Shen W, Shao L, Zeng L, Huang X, *et al*. The Synergism of Natural Compounds and Conventional Therapeutics against Colorectal Cancer Progression and Metastasis. *Frontiers in Bioscience-Landmark*. 2022; 27: 263.
- [10] Lugli A, Zlobec I, Berger MD, Kirsch R, Nagtegaal ID. Tumour budding in solid cancers. *Nature Reviews. Clinical Oncology*. 2021; 18: 101–115.
- [11] Xue C, Du Y, Li Y, Xu H, Zhu Z. Tumor budding as a predictor for prognosis and therapeutic response in gastric cancer: A mini review. *Frontiers in Oncology*. 2023; 12: 1003959.
- [12] Liu M, Yang J, Xu B, Zhang X. Tumor metastasis: Mechanistic insights and therapeutic interventions. *MedComm*. 2021; 2: 587–617.
- [13] Zlobec I, Lugli A. Tumour budding in colorectal cancer: molecular rationale for clinical translation. *Nature Reviews. Cancer*. 2018; 18: 203–204.
- [14] Shivji S, Cyr DP, Pun C, Duan K, Sari A, Tomin R, *et al*. A Novel Combined Tumor Budding-Poorly Differentiated Clusters Grading System Predicts Recurrence and Survival in Stage I-III Colorectal Cancer. *The American Journal of Surgical Pathology*. 2022; 46: 1340–1351.
- [15] Ji W, Zhao R, Lin X, Shao S, Lu S, Cai R, *et al*. Comprehensive Analysis of Competing Endogenous RNA Network in T3 Colorectal Cancer Lymph Node Involvement. *Journal of Biological Regulators and Homeostatic Agents*. 2022; 36: 463–472.
- [16] Müller F, Lugli A, Dawson H. Tumor budding in colorectal cancer-Information for clinical use and instructions for practical evaluation. *Der Pathologe*. 2022; 43: 45–50.
- [17] De Smedt L, Palmans S, Andel D, Govaere O, Boeckx B, Smeets D, *et al*. Expression profiling of budding cells in colorectal cancer reveals an EMT-like phenotype and molecular subtype switching. *British Journal of Cancer*. 2017; 116: 58–65.
- [18] Liu J, Xiao Q, Xiao J, Niu C, Li Y, Zhang X, *et al*. Wnt/ β -catenin signalling: function, biological mechanisms, and therapeutic opportunities. *Signal Transduction and Targeted Therapy*. 2022; 7: 3.
- [19] Liu J, Wang Y, Birnbaum MJ, Stoffers DA. Three-amino-acid-loop-extension homeodomain factor Meis3 regulates cell survival via PDK1. *Proceedings of the National Academy of Sciences of the United States of America*. 2010; 107: 20494–20499.
- [20] Sonnet W, Rezsöhazy R, Donnay I. Characterization of TALE genes expression during the first lineage segregation in mammalian embryos. *Developmental Dynamics*. 2012; 241: 1827–1839.
- [21] Elkouby YM, Elias S, Casey ES, Blythe SA, Tsabar N, Klein PS, *et al*. Mesodermal Wnt signaling organizes the neural plate via Meis3. *Development (Cambridge, England)*. 2010; 137: 1531–1541.

- [22] Vlachakis N, Choe SK, Sagerström CG. Meis3 synergizes with Pbx4 and Hoxb1b in promoting hindbrain fates in the zebrafish. *Development* (Cambridge, England). 2001; 128: 1299–1312.
- [23] Uribe RA, Bronner ME. Meis3 is required for neural crest invasion of the gut during zebrafish enteric nervous system development. *Molecular Biology of the Cell*. 2015; 26: 3728–3740.
- [24] Castillo A, Kramer N, Schwartz CE, Miles JH, DuPont BR, Rosenfeld JA, *et al.* 19q13.32 microdeletion syndrome: three new cases. *European Journal of Medical Genetics*. 2014; 57: 654–658.
- [25] Zhang Y, Pan Q, Shao Z. Tumor-Suppressive Role of microRNA-202-3p in Hepatocellular Carcinoma Through the KDM3A/HOXA1/MEIS3 Pathway. *Frontiers in Cell and Developmental Biology*. 2021; 8: 556004.
- [26] Krasnytska DA, Khita OO, Tsybalyk DO, Luzina OY, Cherednychenko AA, Kozynkevich HE, *et al.* The impact of glutamine deprivation on the expression of MEIS3, SPAG4, LHX1, LHX2, and LHX6 genes in ERN1 knockdown U87 glioma cells. *Endocrine Regulations*. 2022; 56: 38–47.
- [27] Green MR, Sambrook J. *Molecular Cloning: A Laboratory Manual*. 4th edn. Cold Spring Harbor Laboratory Press: Cold Spring Harbor, New York. 2012.
- [28] Li C, Tang Z, Zhang W, Ye Z, Liu F. GEPIA2021: integrating multiple deconvolution-based analysis into GEPIA. *Nucleic Acids Research*. 2021; 49: W242–W246.
- [29] Kassambara A, Rème T, Jourdan M, Fest T, Hose D, Tarte K, *et al.* GenomicScape: an easy-to-use web tool for gene expression data analysis. Application to investigate the molecular events in the differentiation of B cells into plasma cells. *PLoS Computational Biology*. 2015; 11: e1004077.
- [30] Smith JJ, Deane NG, Wu F, Merchant NB, Zhang B, Jiang A, *et al.* Experimentally derived metastasis gene expression profile predicts recurrence and death in patients with colon cancer. *Gastroenterology*. 2010; 138: 958–968.
- [31] Gao ZH, Lu C, Wang MX, Han Y, Guo LJ. Differential β -catenin expression levels are associated with morphological features and prognosis of colorectal cancer. *Oncology Letters*. 2014; 8: 2069–2076.
- [32] Gavert N, Ben-Ze'ev A. Epithelial-mesenchymal transition and the invasive potential of tumors. *Trends in Molecular Medicine*. 2008; 14: 199–209.
- [33] Zhou B, Zong S, Zhong W, Tian Y, Wang L, Zhang Q, *et al.* Interaction between laminin-5 γ 2 and integrin β 1 promotes the tumor budding of colorectal cancer via the activation of Yes-associated proteins. *Oncogene*. 2020; 39: 1527–1542.
- [34] Hong Y, Ho KS, Eu KW, Cheah PY. A susceptibility gene set for early onset colorectal cancer that integrates diverse signaling pathways: implication for tumorigenesis. *Clinical Cancer Research*. 2007; 13: 1107–1114.
- [35] Dibner C, Elias S, Ofir R, Souopgui J, Kolm PJ, Sive H, *et al.* The Meis3 protein and retinoid signaling interact to pattern the *Xenopus* hindbrain. *Developmental Biology*. 2004; 271: 75–86.
- [36] Iber D. The control of lung branching morphogenesis. *Current Topics in Developmental Biology*. 2021; 143: 205–237.
- [37] Ngan CY, Yamamoto H, Seshimo I, Tsujino T, Man-i M, Ikeda JI, *et al.* Quantitative evaluation of vimentin expression in tumour stroma of colorectal cancer. *British Journal of Cancer*. 2007; 96: 986–992.
- [38] Elkouby YM, Polevoy H, Gutkovich YE, Michaelov A, Frank D. A hindbrain-repressive Wnt3a/Meis3/Tsh1 circuit promotes neuronal differentiation and coordinates tissue maturation. *Development*. 2012; 139: 1487–1497.
- [39] Steeg PS. Targeting metastasis. *Nature Reviews. Cancer*. 2016; 16: 201–218.
- [40] Ma YQ, Wen Y, Liang H, Zhong JG, Pang PP. Magnetic resonance imaging-radiomics evaluation of response to chemotherapy for synchronous liver metastasis of colorectal cancer. *World Journal of Gastroenterology*. 2021; 27: 6465–6475.
- [41] Li Y, Xing C, Wei M, Wu H, Hu X, Li S, *et al.* Combining Red Blood Cell Distribution Width (RDW-CV) and CEA Predict Poor Prognosis for Survival Outcomes in Colorectal Cancer. *Journal of Cancer*. 2019; 10: 1162–1170.
- [42] Aasebø K, Dragomir A, Sundström M, Mezheyski A, Edqvist PH, Eide GE, *et al.* CDX2: A Prognostic Marker in Metastatic Colorectal Cancer Defining a Better *BRAF* Mutated and a Worse *KRAS* Mutated Subgroup. *Frontiers in Oncology*. 2020; 10: 8.
- [43] Govaere O, Petz M, Wouters J, Vandewynckel YP, Scott EJ, Topal B, *et al.* The PDGFR α -laminin B1-keratin 19 cascade drives tumor progression at the invasive front of human hepatocellular carcinoma. *Oncogene*. 2017; 36: 6605–6616.